THE JOURNAL OF PHYSICAL CHEMISTRY Letters

LETTER

pubs.acs.org/JPCL

Theoretical Study of Coherent Excitation Energy Transfer in Cryptophyte Phycocyanin 645 at Physiological Temperature

Pengfei Huo[†] and David F. Coker[*,†,‡]

[†]Department of Chemistry, Boston University, 590 Commonwealth Avenue, Boston, Massachusetts 02215, United States

[‡]Department of Physics, and Complex Adaptive Systems Laboratory, University College Dublin, Belfield, Dublin 4, Ireland

Supporting Information

ABSTRACT: Recent two-dimensional photon-echo experiments suggest that excitation energy transfer in light harvesting systems occurs coherently rather than by incoherent hopping. The signature quantum beating of coherent energy transfer has been observed even at ambient temperatures. In this letter, we use an iterative linearized density matrix (ILDM) propagation approach to study this dynamics in a realistic multistate system−bath model. Our calculations reproduce the observed 400 fs decoherence time, and studies that vary the system Hamiltonian and structured spectral density describing the chromophore network−protein environment interactions give results that enable us to explore the role of initial coherence in energy transfer efficiency of the model network. Our findings suggest that the initial coherence has only a slight effect on energy transfer in this model system. We explore energy transfer optimization of different chromophores in the network by controlling environmental properties. This study points to the importance of stochastic resonance behavior in determining optimal network throughput.

SECTION: Dynamics, Clusters, Excited States

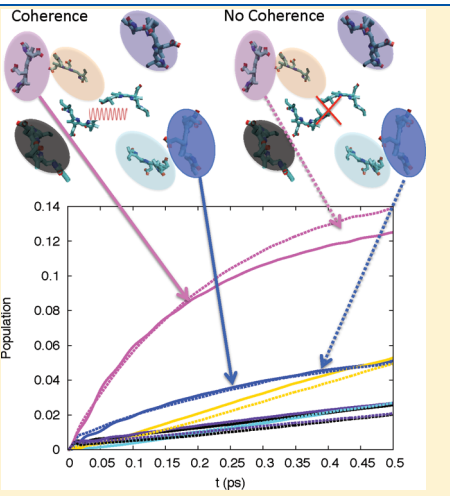

Recent multidimensional nonlinear spectroscopic experiments[1−4] have demonstrated that the early stages of photoexcitation and excitation energy transfer in various photosynthetic light harvesting complexes involve relatively long-lived coherent quantum dynamics in which the energy moves through these quantum networks via processes that are characterized by a balance of coherent beating of the amplitudes of the different excited chromophore states and dissipative relaxation from higher to lower energy states. The mechanism suggested by these observations is in stark contrast to the purely incoherent hopping mechanism that has been assumed in standard models of this process for decades. Remarkably, in these systems, the spectroscopic signature of coherent excitation energy transfer dynamics, observed as oscillatory beating features in nonlinear optical signals that are related to the electronic coherence, are even found at ambient temperatures[1,2] where such quantum coherent behavior is usually expected to be damped out.

These light harvesting systems, such as phycocyanin PC645 from Chroomonas CCMP270[1], which we discuss in this letter, involve assemblies of several chromophores, arrayed in structured complexes embedded in a protein scaffolding as displayed in the left panel of Figure 1. The site electronic excitation energies and principle electronic couplings between sites that characterize the system Hamiltonian, H_S, employed in these model studies are displayed in the right panel of Figure 1. (Details of the H_S used in these studies, whose site energies are obtained from experimental spectra,[5] and couplings from electronic structure calculations[1] can be found in Table S.1 of the Supporting Information). Over the past few years, model Hamiltonians of this type, which also include environmental interactions, have been parametrized for a variety of light harvesting chromophore networks and, as we will demonstrate in the calculations reported in this paper, they can provide realistic models that capture the important features of the coherent quantum dynamics that are observed in the ultrafast nonlinear optical experiments. There are several generic elements of these model system Hamiltonians that are apparent in the energy level connectivity diagram presented in the right panel of Figure 1. These ubiquitous elements include: clusters of chromophores with closely spaced excitation energies that have appreciable electronic couplings between the cluster members such as, for example, the chromophore dimers linked by the red paths in Figure 1; chromophore states whose excitation energies are isolated but which exhibit appreciable electronic coupling to neighboring states; and finally these isolated but coupled states are often arranged energetically in cascade or barrier patterns that funnel or rectify the directional flow of energy through these multichromophore networks, and toward reaction centers (in this case, on the outskirts of the chromophore network).

Natural light harvesting antenna complexes show enormous diversity in structure;[6] for example, some are exquisitely

Received: March 5, 2011
Accepted: March 11, 2011
Published: March 18, 2011

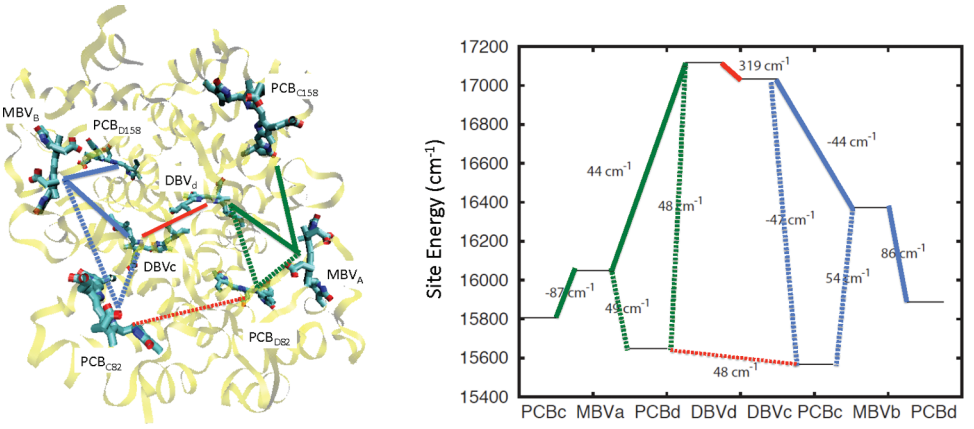

Figure 1. Left panel: Structure of phycocyanin PC645 showing predominately α-helical protein scaffolding with embedded bilin chromophores. Lines connect chromophores that participate in various coherences observed in the dissipative quantum dynamics of the system (see text). Right panel: Energy level "connectivity diagram" for PC645. Horizontal line segments give site energies in cm^{-1} of chromophore sites listed along the *x*-axis. Lines connecting the ends of these site energy levels are labeled with the major off-diagonal electronic couplings between sites. The color coding is consistent with structural connections in the left panel.

symmetrical, while in other systems the chromophores sit in loosely structured arrangements in the protein support matrix. Even something as basic as interchromophore separation shows strong variation; for example, in organisms with chlorophyll-based networks, the typical interchromophore spacing is ∼1 nm, while in organisms with bilin-based networks, like the system considered here, the interchromophore spacing can be more than ∼2 nm, yet the network harvesting efficiencies are always close to 100%. Nevertheless, the key elements of the chromophore excitation energy/electronic coupling landscape, outlined above, are preserved across this diversity of harvesting network structure. Thus, despite this variability in structure, the mechanism of excitation transport seems to be ubiquitous and it has been suggested that the relatively long-lived coherent dynamics observed in ultrafast nonlinear optical spectroscopy signals perhaps plays a role in the highly efficient solar energy capture and transfer in these systems that funnel electronic excitation into reaction centers where long-term energy storage is initiated.

Reliable modeling of this coherent excitation energy transfer in these light harvesting chromophore networks presents a significant challenge to conventional theoretical approaches such as Förster resonance energy transfer (FRET) theory,[7,8] or employing the Redfield[9,10] or Lindblad equations,[11,12] which can in some situations, provide inaccurate descriptions of these processes due to various approximations employed (e.g., use of perturbation theory,[13] the incoherent transfer approximation,[7] the markovian approximation,[13−16] and the secular approximation[11,15,16]) that can limit their applicability when treating realistically parametrized models of light harvesting complexes.

The limitations of many of these approximations and the shortcomings for the particular application to photosynthetic light harvesting networks have been discussed elsewhere.[14] To overcome these limitations of the conventional methods within this context, various efforts have been made by a number of authors; for example, Jang and Silbey and co-workers developed a multichromophore version of FRET theory[7,8] that they applied to LHII. Ishizaki and Fleming extended a hierarchical coupled reduced master equation[16−18](HCRME) approach to study coherent excitation energy transfer in the Fenna−Matthews−Olsen (FMO) complex. Recent calculations on the PC645 complex[19] employ the generalized Bloch−Redfield (GBR) equation approach that can also describe non-Markovian quantum dissipative dynamics. The present authors used the iterative linearized density matrix (ILDM) propagation approach[14] to conduct benchmark comparisons with results from the HCRME approach, the linearized semiclassical initial value representation (LSC-IVR)[20] approach, as well as methods that incorporate various improvements to Redfield theory.[10,21−23] We showed[14] that the ILDM approach is a powerful method that can handle nonmarkovian dynamics in systems with general spectral densities describing the system−bath coupling, and system Hamiltonian forms, and thus can be reliably applied beyond the limits of many of the competitor approaches.

In this letter we report results obtained using the ILDM propagation approach[24−27] to study a model of phycocyanin PC645 from Chroomonas CCMP270 at ambient temperature (T = 294K). PC645 contains eight bilin molecules covalently bound to the protein scaffold[1] (see left panel of Figure 1). A dihydrobiliverdin (DBV) dimer is located at the center of the complex. Excitation of this dimer initiates the harvesting process. The electronic coupling[1] between the closely spaced DBVc and DBVd molecules is about 320 cm^{-1}, and this relatively strong coupling results in delocalization of the excitation yielding the dimer excited electronic eigenstates of the bare system Hamiltonian. These eigenstates of H_S form the basis of exciton states, and the initially excited dimer states, for example, are labeled DBV$_+$ and DBV$_-$. Our numerical simulations with this model show strong coherent oscillations in the populations of the states making up the DBV dimer, and the off-diagonal coherence density matrix elements in the exciton basis show similar oscillations and decay, consistent with experimental observations of long-lived coherence found in ultrafast nonlinear multidimensional spectroscopy signals.[1]

It is important to note that our calculations cannot reproduce the detail of the low frequency oscillatory features discernible in the experimental signals as we employ a very simplified model for the bath, and the spectral density describing the coupling between the system and bath. As detailed below, our model includes a non-Markovian structured spectral density with a broad high frequency peak, and a sharper low frequency feature, and we will

dx.doi.org/10.1021/jz200301j |*J. Phys. Chem. Lett.* 2011, 2, 825–833

explore the sensitivity of our results to changing the relative importance of these gross features. To correctly reproduce all the oscillatory features observed in the experimental results, we would need a more detailed model including, for example, explicit Brownian oscillator modes to represent the effects of underdamped environmental vibrations on the signals.[4] The effects of these types of motions on the density matrix dynamics will be explored elsewhere (in preparation).

These calculations of the dynamics of energy transfer in this dissipative model system indicate that the significant electronic interactions of each member DBV molecule with it is neighbor mesobiliverdin (MBV) acceptor chromophores, and the proximity of the excitation energies of these states results in excitation energy transfer between these molecules. In fact, the couplings between all the molecules result in rapid energy transfer throughout the harvesting network. The goal of this paper is to explore the efficiency of this network excitation energy transfer and how it is influenced by various properties of the spectral density describing the interactions of the chromophores with their fluctuating environment. The coupling to the environment, for example, influences the quantum coherent dynamics of the excitation energy transfer, and we will explore the effects of fluctuations and dissipation on the role played by such quantum dynamical effects and their influence on excitation energy transfer and localization in such multichromophore networks.

Our calculations also show evidence of a coherent excitation energy transfer cascade through the intermediate MBV molecules to the lower energy PCB acceptor chromophores as excitation energy migrates out to the periphery of the harvesting network. The model gives long-lived oscillations in off-diagonal density matrix elements for these different states that qualitatively decay on time scales consistent with experimental observations, although a more detailed model of the coupling to specific bath modes would be needed for a more quantitative description of these dynamics. By varying the shape of the spectral density and the overall strength of the system−bath coupling, we explore how such effects influence the rate of energy transfer through the harvesting network and suppress or enhance its energy transfer efficiency.[2] The aim of this letter is to use accurate quantum dynamical simulation methods to explore the suggestion that the observed long-lived quantum coherent dynamics involving beating between coupled states of chromophore clusters plays a role in the efficient functioning of these networks. Our approach will involve varying the properties of the quantum subsystem−bath interaction in an effort to learn whether the presence of coherent quantum beating provides a mechanism to optimize excitation energy throughput in these networks.

Model Calculations. The ILDM propagation scheme used in the calculations described in this letter involves iterating a short time approximation to the multistate quantum subsystem−continuous environment propagator and, as mentioned earlier, can be applied beyond standard perturbation theory and Markovian approximations. The scheme is outlined in the Supporting Information. For a detailed description of tests and implementation of the approach, we refer the reader to the published literature.[24,27]

The model Hamiltonian used in the calculations reported in this letter to describe the PC645 light harvesting complex has a quantum subsystem component, H_S, that contains only system operators, and the system−bath coupling term, H_{SB} that contains both system and bath quantities. In this model of the system−bath coupling terms, each chromophore experiences dissipative interactions with its own independent bath, thus the general Hamiltonian has the following form:

$$\begin{aligned}\hat{H}_{\mathrm{indep}}^{\mathrm{PC645}} &= H_S + H_{SB} \\ &= \sum_{\alpha=1}^{N_{\mathrm{state}}} \left\{ \varepsilon_\alpha + \sum_{l=1}^{n^{(\alpha)}} c_l^{(\alpha)} x_l^{(\alpha)} + \sum_{\beta=1}^{N_{\mathrm{state}}} \sum_{m=1}^{n^{(\beta)}} \frac{1}{2}[p_m^{(\beta)2} \right. \\ &\quad \left. + \omega_m^{(\beta)2} x_m^{(\beta)2}] \right\} |\alpha\rangle\langle\alpha| + \sum_{\alpha<\beta}^{N_{\mathrm{state}}} \Delta_{\alpha,\beta}[|\alpha\rangle\langle\beta| + |\beta\rangle\langle\alpha|] \end{aligned} \quad (1)$$

The electronic Hamiltonian, H_S, is determined by the diagonal electronic site energies,[5] ε_α, of the chromophores, and the off-diagonal electronic couplings between the chromophores,[1,28] $\Delta_{\alpha,\beta}$. The site energies, connected by the lines joining sites with the largest couplings (given in cm^{-1}), for this model are displayed in the right panel of Figure 1. The full set of parameters defining H_S are summarized in the Supporting Information.

The spectral densities, $j^{(\alpha)}(\omega)$, for each chromophore's independent bath of harmonic oscillators, that are bilinearly coupled to the chromophore, have the structured Debye cutoff ohmic form[5,19] $j^{(\alpha)}(\omega) = j(\omega) = 2\lambda_0\{\omega\tau_1[(\omega\tau_1)^2 + 1]^{-1} + \omega\tau_2[(\omega\tau_2)^2 + 1]^{-1}\}$ where the parameter λ_0 equals 130 cm^{-1}. The "solvent reorganization energy" is defined as $\lambda = 1/\pi\int_0^\infty d\omega j(\omega)/\omega = 2\lambda_0$. This quantity controls the overall strength of the interaction between each quantum subsystem and its bath. The bath relaxation times, $\tau_1 = 50$ fs and $\tau_2 = 1.5$ ps, adjust the range of frequencies or time scales on which the baths can respond.

This spectral density, which determines the bath coupling constant strengths $c_l^{(\alpha)}$ according to $j^{(\alpha)}(\omega) = (\pi/2)\Sigma_l^{n(\alpha)}(c_l^{(\alpha)2}/\omega_l^{(\alpha)})\delta(\omega-\omega_l^{(\alpha)})$, is plotted in the left panel of Figure 2, where we observe the key structure of this system−bath interaction model, i.e., distinct peaks at high and low frequencies that result in highly non-Markovian quantum dissipative dynamics.

In earlier studies[14] exploring the accuracy of the linearized short time approximation that underlies the ILDM approach, we found that the linearized scheme (no iteration; the so-called linearized approach to nonadiabatic dynamics in the mapping formulation, or LAND-map approach[25,26]) provided reliable density matrix propagation results for times on the order of 1 ps for systems with electronic couplings and site excitation energies on the order of those outlined above, provided that the bath relaxation times were sufficiently long. For a fast relaxing bath (e.g., $\tau_c \sim 100$ fs), the linearized approach provides a reasonable representation of the coherent oscillations in populations, but it fails to reproduce accurate thermalization of the populations at long times. However, for slower baths (say, $\tau_c \sim 500$ fs), the approach is surprisingly accurate. These observations are born out in our findings for the PC645 system presented in the right panel of Figure 2, where results obtained with ILDM (10 hop attempts in 0.5 ps) and LAND-map propagations are compared for a reduced four-state model containing only the chromophores DBVc, DBVd, MBVa, and MBVb. The linearized calculations show excellent agreement with the benchmark results obtained with ILDM propagation as expected since this system is characterized by a long relaxation time, $\tau_2 = 1.5$ ps. Consequently, throughout the remainder of this paper, we present results calculated using the linearized approach, as this method requires considerably less computation to obtain converged and reliable results.

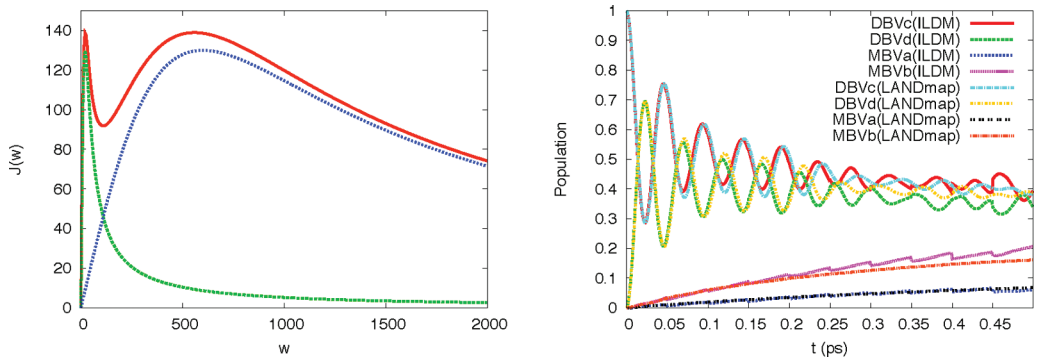

Figure 2. Left panel shows the components of the spectral density use in this paper. They include two different components with the Debye cutoff ohmic form: a fast relaxing component with τ_1 = 50 fs (blue) and a much slower component with τ_2 = 1.5 ps (green). The total spectral density is represent by the solid red curve. The units for ω and $J(\omega)$ are cm^{-1}. The right panel presents a comparison between populations computed using ILDM and LAND-map. The labeled curves give the ILDM results with 10 hop attempts in 500 fs, and the rest of the curves give the LAND-map results.

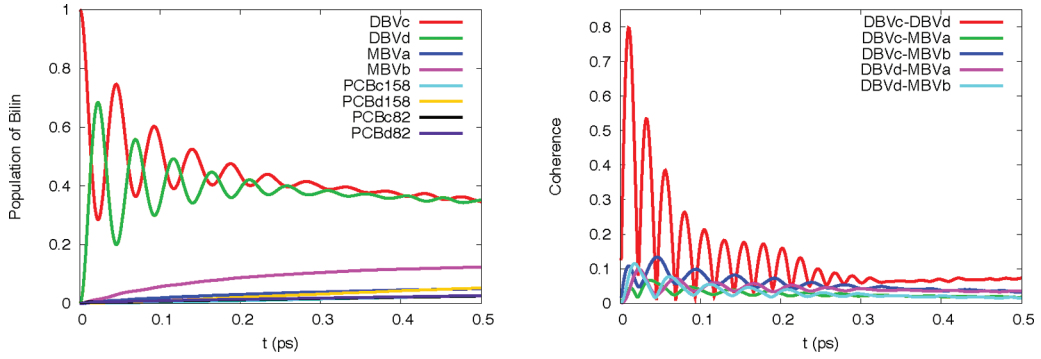

Figure 3. Populations, ρ_{ii} (left panel) and absolute value of the off-diagonal or coherence density matrix elements, plotted as $2|\rho_{ij}^{\text{site}}|$ (right panel), in the site representation for PC645 at T = 294K. Excitation is initially localized on the DBVc chromophore.

The left panel of Figure 3 presents the site population dynamics for the full eight state model of PC645 after initial excitation of the DBVc chromophore at T = 294K. Coherent beating of the populations of the DBVc and DBVd chromophores that form a strongly coupled dimer with closely spaced energies (see right panel of Figure 1) is observed beyond 400 fs. The populations of the other bilin chromophores in the complex, however, grow in more smoothly.[14,17] The right panel of Figure 3 shows the dynamics of the absolute values of the main off-diagonal decoherence density matrix elements in the site basis where we observe oscillation out to about 400 fs and constant plateau values beyond this time.[14]

A careful examination of the populations of the intermediate and peripheral chromophores (see bottom left panel of Figure 4 where we present the minor population data from the left panel of Figure 3 on an expanded scale) suggests that, even though the initial dimer sites are more or less equally populated by the coherent beating, the excitation evolves preferentially along one of the possible pathways through the chromophore sites of the complex. Thus, for example, the MBVb site population grows in much faster than that of the MBVa site, which is more widely separated in energy from the DBV dimer (see right panel of Figure 1). The significant population in MBVb preferentially feeds population to the PCBd158 and PCBc82 sites. The chromophores PCBc82 and PCBd82 on opposite sites of the complex are very close in energy, and electronically coupled (~48 cm^{-1}), so we find that their populations, although small initially, grow in essentially on top of one another and, just like the DBV dimer, they too show evidence of early cooperative coherent beating. The population in either of these two sites is larger than that of the PCBc158 site that terminates the minor path running through the sites on the left-hand side of the site connectivity diagram in the right panel of Figure 1. Thus the paths running through the sites on the right-hand side of the connectivity diagram dominate in rapidly distributing excitation energy among the accessible chromophores.

In the Supporting Information, we present the results of model calculations that explore the different dynamics arising from the various pathways depicted in Figure 1 by selectively exciting the different MBVa and MBVb intermediate states initially.

In the upper panels of Figure 4, we plot the dynamics of various off-diagonal density matrix elements in the exciton basis defined by diagonalizing H_S. In this representation, the off-diagonal density matrix elements vanish on the decoherence time scale and thus show behavior that is more readily compared to the experimental signals than the site basis coherence results in the right panel of Figure 3.[14] The dynamical behavior of the off-diagonal elements in the exciton basis thus gives a clearer picture of the decoherence time scales.

The results in Figure 4 were again obtained with chromophore DBVc initially excited. Those presented in the left-hand column were obtained from calculations that employed the full double peaked spectral density shown in the left panel of Figure 2. Results in the right-hand column of Figure 4, on the other hand, were obtained

dx.doi.org/10.1021/jz200301j |J. Phys. Chem. Lett. 2011, 2, 825–833

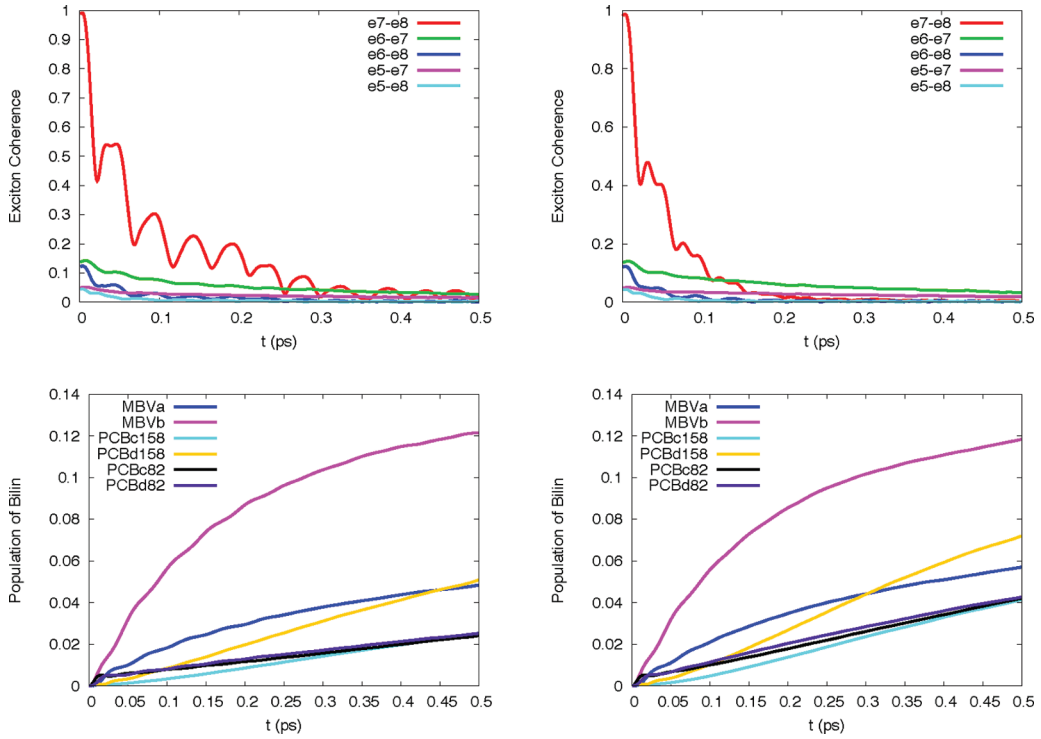

Figure 4. Effects of structured spectral density on time dependence of density matrix elements. Top panels compare off-diagonal coherence density matrix elements (plotted as $2|\rho_{ij}^{exe}|$) computed in the exciton basis for PC645 initially excited to site DBVc at $T = 294$K. Upper left panel shows coherence results for the fully structured spectral density that includes both low and high frequency components. Panels in the right column give results for a spectral density that contains only the broad high frequency peak with amplitude adjusted to give same reorganization energy as with the fully structured spectral density. Bottom panels present site basis state populations for the same calculations with these different spectral densities.

by removing the low frequency peak from the spectral density and renormalizing the magnitude of the new spectral density to preserve the value of the solvent reorganization energy (see below).

The exciton states are labeled e1 to e8, with increasing excitation energy. Excitons e7 and e8 are mainly composed of DBV_- and DBV_+, i.e., antisymmetric and symmetric linear combinations of the DBV sites, though they also contain small contributions from the other bilin sites. The time dependence of the off-diagonal coherence matrix elements (here plotted as $2|\rho_{ij}^{exe}|$) in the exciton basis displayed in the upper left panel of Figure 4 shows evidence of long-lived quantum coherent dynamics of the DBV_+/DBV_- coherent superposition state that is initially excited in the experiments (see Supporting Information for details). The magnitude of the off-diagonal density matrix element, $|DBV_+\rangle\langle DBV_-|$, (i.e., $|e7\rangle\langle e8|$) is related to the contribution of this coherence to the signal that is probed in nonlinear optical spectroscopy experiments,[1] and our calculations with the full spectral density thus give a time scale for decay of this quantum coherence of ~400 fs, reproducing the basic features observed in the experimental results. The other coherences displayed in this figure, e.g., $|e6\rangle\langle e7|$, which are dominated by the MBVb−DBV_+ linear combination, similarly show persistence of coherent beats between these states that involve sites separated by large distances (~25 Å) in these complexes. The relaxation times of the amplitudes of the off-diagonal density matrix elements computed in the exciton basis provide reasonable estimates of the decoherence times obtained in the photon echo experiments. The relationship between observed decoherence times and representation has been discussed in the context of photosynthetic light harvesting elsewhere (in preparation).

The upper right panel in Figure 4 shows the same exciton coherence elements but now computed for a spectral density that contains only the high frequency component. For the results of the calculation reported in the right-hand column of Figure 4, the magnitude of the high frequency part of the spectral density has been adjusted to maintain the value of the solvent reorganization energy of the full structured spectral density. Thus $J_{high}(\omega) = 4\lambda_0\omega\tau_1/[(\omega\tau_1)^2+1]$. We see that the decoherence time scale for the $|e7\rangle\langle e8|$ coherence, for example, in the presence of only this high frequency bath component is a factor of 2 faster than that for the full spectral density (upper left panel), suggesting that low frequency modes may play a significant role in extending decoherence times in these systems as speculated in earlier work.[5,14,16,17] The results presented in this figure, however, indicate that the other exciton coherence elements, e.g., $|e6\rangle\langle e7|$, or $|e5\rangle\langle e7|$, etc., have decoherence times that are insensitive to removing the low frequency component of the spectral density (see Supporting Information for details). Also in the Supporting Information, we present the real and imaginary parts of ρ_{78}^{exe} and observe the effects of the different bath characteristics on this example coherence density matrix dynamics.

In the bottom panels of Figure 4 we compare the site population dynamics for the same runs whose exciton coherences are displayed in the top panels. The time dependence of the site populations give information about the rate at which the excitation is delocalized throughout the network from the initially excited strongly coupled dimer states to the peripheral sites at the edge of the network. The lower left panel shows site populations for the full structured spectral density, including low and high frequency modes, while in the right panel we present the

dx.doi.org/10.1021/jz200301j |J. Phys. Chem. Lett. 2011, 2, 825–833

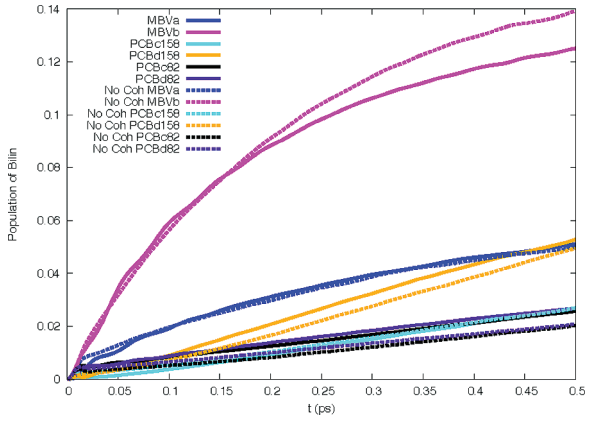

Figure 5. Comparison of populations of peripheral acceptor chromophores as functions of time when the initially excited, coherently coupled DBV dimer states are replaced with a single effective mean state, removing initial coherence. Results for fully structured spectral density at $T = 294$ K are presented. Solid curves give site populations observed with coherently coupled DBV dimer initial states; dashed curves show site populations obtained when initial mean DBV state is used.

site populations including only the high frequency component of the spectral density having removed the low frequency modes and renormalized as outlined above.

Comparing the site population results presented in the lower left panel for the full double peaked spectral density with those in the lower right panel obtained with just the broad higher frequency peak, we see that the presence of the low frequency modes that prolong the exciton coherence lifetime as we saw above actually *slows* the rate of excitation energy transfer out to the peripheral chromophores. This is clearly seen, for example, for the low energy coupled dimer states PCBc82 and PCBd82, which, in the presence of only the high frequency part of the spectral density (bottom right panel), grow in at about twice the rate of the same sites when the full spectral density is employed (bottom left panel). It is interesting to note, in contrast, that the rate of growth of the populations of intermediate or "conduit" states, e.g., the MBVb site, are apparently not effected much by removing the low frequency peak in the spectral density.

In order to directly explore the effect of the initially prepared coherent superposition of DBV dimer states on the rate of energy transfer to the peripheral chromophore acceptor states, we ran exploratory calculations with a Hamiltonian in which the DBV dimer states were replaced by a single state with excitation energy that was the mean of the DBV site energies and which had the same coupling strengths to the rest of the chromophore network and to the environment. In Figure 5 we compare the populations of the peripheral acceptor chromophores as functions of time computed in the presence of the fully coherently coupled DBV dimer states (solid curves), with the populations obtained when the DBV dimer is replaced by a single "mean state" where there can be no initially excited coherence. From the figure it is apparent that the principle intermediate MBVb state builds up slightly more population in the absence of coherence (dashed magenta curve) and so it passes on slightly less population to the PCB acceptor states. Thus it is apparent that the presence of the initially excited coherent superposition of DBV dimer states does enhance the energy transfer rate to these peripheral PCB acceptor states, though the effect is very slight. Note, for example, that the solid gold, black and purple curves (with coherent Hamiltonian structure) are slightly above the associated dashed curves (without coherent Hamiltonian structure) at longer times.

To explore the influence of system−environment coupling strength on excitation energy transfer rates between chromophores in the PC645 light harvesting network, we conducted a series of calculations in which we varied the solvent reorganization energy with the fully structured model spectral density at $T = 294$ K. In Figure 6 we display the time-dependent site populations for different chromophores in the network. The apparently ubiquitous behavior observed in the various panels of this figure shows an optimization of asymptotic population with varying solvent reorganization parameters measured in multiples of $\lambda = 260\ \mathrm{cm}^{-1}$. For the initially occupied dimer state, DBVc, (upper left panel) for example, we see that the coherently oscillating trace for solvent reorganization energy = λ arrives at about 0.35 at $t = 0.5$ ps. As the reorganization energy is increased to 5λ, however, the coherent oscillation gives way to overdamped relaxation, and the population arrives finally at a value of 0.3. For higher reorganization energy values (e.g., 10, 20, and 50λ), the terminal population of this initial state steadily increases as the efficiency of energy transfer to the surrounding network of chromophores decreases with the increased coupling to the environment. Thus the energy transfer from the donor states is found to be optimized at about 5λ.

Of course an opposite, maximization trend with solvent reorganization energy is observed for the populations of the peripheral acceptor chromophores in the remaining panels of Figure 6. For example, in the lower right panel we see that the terminal population of the PCBc82 chromophore increases as the reorganization energy is increased from 0 to 10λ. Beyond this, however, the terminal population decreases by more than a factor of 2 as the solvent reorganization is increased to 50λ. Depending on their location and role in the network, different chromophores show terminal maximization of population at different values of the solvent reorganization energy. For example, the intermediate MBVb chromophore (upper right panel of Figure 6) shows coherent population oscillation at zero coupling, then maximizes at very low values of solvent reorganization energy around λ, and subsequently decreases by nearly a factor of 5 as the solvent reorganization is increased to 50λ.

This type of optimization behavior with increasing system bath coupling strength has been observed in simple models of light harvesting networks treated with approximate analytic theories, for example, in the work of Plenio and co-workers,[29−31] and others.[19,32] These authors describe this behavior in terms of the ideas underlying stochastic resonance phenomena: For a pair of sites whose static excitation energies are separated by $\varepsilon_{\alpha,\beta}$ with small electronic coupling $\Delta_{\alpha,\beta}$, say, if the solvent reorganization energy is weak, the fluctuations in the site energies driven by the bath dynamics will be small compared to the electronic excitation energy gap and there will be little population transfer. As the system−bath coupling is increased and the fluctuations in site energies become on the order of the static excitation energy gap there will be many times when the fluctuations drive the site energies into resonance and the finite electronic coupling will lead to appreciable population transfer and maximization of the energy transfer rate between the sites for some value of system −bath coupling. At stronger system−bath coupling still, the larger fluctuations in site energies drive the system out of resonance more often, and we see a decrease in population transfer in the network. The fact that the results presented in Figure 6 reveal precisely these signatures of stochastic resonance behavior in this

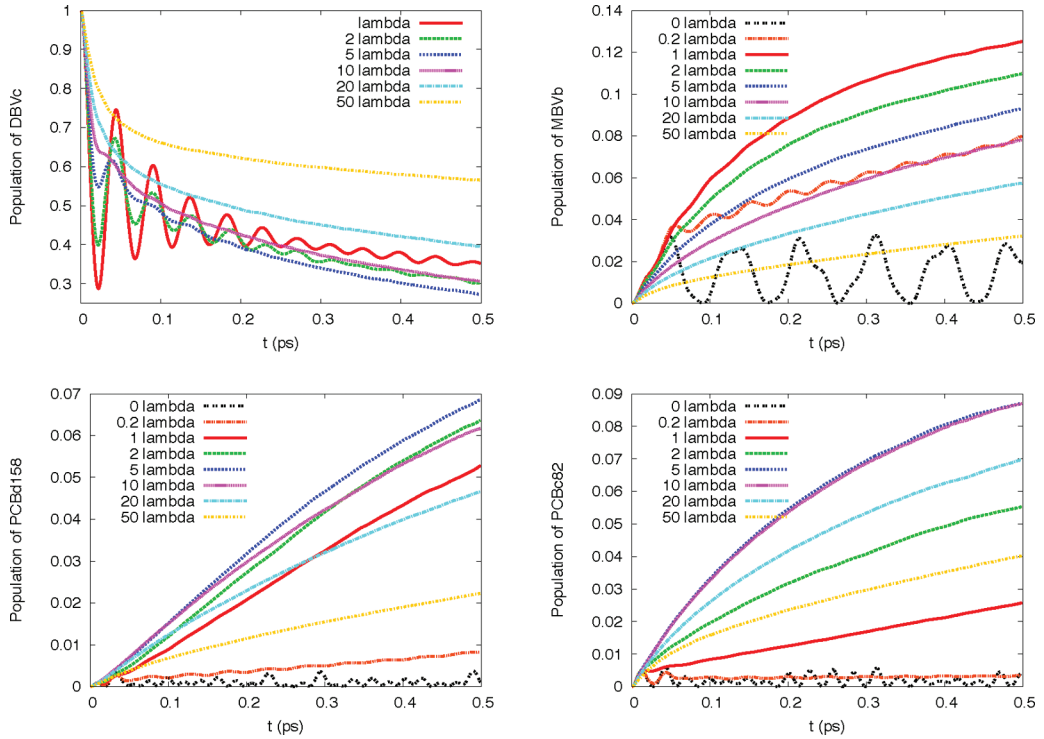

Figure 6. Populations of different chromophore states as functions of time after initial excitation of the DBVc site. Each panel presents results for a different chromophore in the network, and explores the influence of the strength of system bath coupling as characterized by the solvent reorganization energy parameter, λ, on the site population dynamics. Results are presented for the full dual peaked spectral density though the characteristic stochastic resonance optimization behavior is also observed with the simplified single peak spectral density. The different traces in each panel all show evidence of a nonmonotonic dependence of the rate of excitation energy transfer from the initial DBVc state, and to the different chromophore states in the network as measured, for example, by the populations at $t = 0.5$ ps.

realistic, non-Markovian model with an accurate treatment of the quantum dynamics is suggestive that the simple ideas underlying the phenomenon of stochastic resonance are robust in determining the optimization behavior of these nanostructured quantum dynamical light harvesting network systems.

With the model system−bath Hamiltonian and the fully structured spectral density including low and high frequency peaks we observe long-lived coherent beating between initially excited coupled chromophore dimer states that decays on a decoherence time scale that is consistent with experimental results for the PC645 system. Due to asymmetry in the energy gap structure of the model employed in these studies, excitation energy initially flows down only one side of the harvesting complex but, due to the presence of a resonant coupled dimer accessed at low energy, the excitation is still able to delocalize and explore both sides of the complex as a result of an effective "coherent short circuit" arising from this low energy resonant coupled dimer.

Our study varying the shape of the spectral density while keeping the overall solvent reorganization energy fixed in this model shows that removing low frequency modes from the model double peaked spectral density can cause more rapid decoherence of the beating between the initially prepared superposition of excited states. In this system, however, we find that the changes in the spectral density outlined above, in which we remove the low frequency peak and couple the remaining high frequency modes more strongly to the system to preserve the overall solvent reorganization energy that leads to the observed more rapid decoherence, also result in faster dissipation of the initial excitation and lead to more rapid deposition of excitation in the peripheral chromophore states. Thus in this model, more rapid decoherence and dissipation brought about by appropriate engineering of the spectral density actually enhances the efficiency of energy transfer in the network.

Our studies in which we re-engineer the model system Hamiltonian, H_S, replacing the initial coherently excited dimer structure by a single "mean state", thus removing even the possibility of initially excited coherence, show that there is very little difference in the ability of the model network to transfer excitation energy to its peripheral states in the presence or absence of coherently excitable structures in the model system Hamiltonian. We thus conclude that, at least for this model of PC645 with its independent, uncorrelated baths for the different chromophores, the coherence that is initially excited in the experiments plays only a small role in the energy transfer properties of the network.

Finally our realistic model calculations and accurate treatment of dynamics have verified the importance of stochastic resonance behavior in this model quantum network. We have seen that different chromophores that play different roles in the network, e.g., intermediates, barrier states, states involved in energy cascades through the network, resonantly coupled dimer quantum communication channel states, and so forth, exhibit different stochastic resonance optimization environmental parameter values. This observation suggests that the local protein environment around different chromophores may be tuned to influence network throughput in controllable ways. Combining these effects arising from stochastic resonance phenomena, with the potential for building in correlated environmental motions[19,33,34] by local

dx.doi.org/10.1021/jz200301j |J. Phys. Chem. Lett. 2011, 2, 825–833

mutation, for example, may provide ways to effectively engineer environments in these quantum energy transport networks to enhance desired properties.

One of the most important features of the linearized, or iterative linearized scheme used to perform the calculations outlined in this paper is that these approaches can, in principle, handle arbitrary model Hamiltonians and spectral densities. As we have demonstrated, structure in the spectral density can have a significant effect on decoherence times and quantum network energy transfer properties in the parameter ranges appropriate for photosynthetic systems. These methods are already proving to be invaluable tools for analyzing the behavior of these complex networks and providing an understanding of how they might be engineered to enhance their desired functionality.

■ ASSOCIATED CONTENT

Supporting Information. Overview of ILDM propagation approach; summary of model system Hamiltonian parameters; exploratory study of energy transfer pathways in PC645; and study of dependence of coherence density matrix elements on model spectral density. This material is available free of charge via the Internet at http://pubs.acs.org.

■ AUTHOR INFORMATION

Corresponding Author
*Electronic mail: coker@bu.edu

■ ACKNOWLEDGMENT

We gratefully acknowledge support for this research from the National Science Foundation under Grant CHE-0911635 and support from Science Foundation Ireland under Grant Number 10/IN.1/I3033. D.F.C. acknowledges the support of his Stokes Professorship in Nanobiophysics from Science Foundation Ireland. We both appreciate discussions with Prof. G. Scholes that led directly to the main ideas explored in this paper. We also acknowledge a grant of supercomputer time from Boston University's Office of Information Technology and Scientific Computing and Visualization as well as an allocation of supercomputing resources from the Irish Center for High End Computing (ICHEC). Thanks Niles.

■ REFERENCES

(1) Collini, E.; Wong, C. Y.; Wilk, K. E.; Curmi, P. M. G.; Brumer, P.; Scholes, G. D. Coherently Wired Light-Harvesting in Photosynthetic Marine Algae at Ambient Temperature. *Nature* **2010**, *463*, 644–648.

(2) Panitchayangkoona, G.; Hayes, D.; Fransted, K. A.; Caram, J. R.; Harel, E.; Wen, J.; Blankenship, R. E.; Engel, G. S. Long-Lived Quantum Coherence in Photosynthetic Complexes at Physiological Temperature. *Proc. Natl. Acad. Sci. U.S.A.* **2010**, *107*, 12766–12770.

(3) Engel, G. S.; Calhoun, T. R.; Read, E. L.; Ahn, T.-K.; Mancal, T.; Cheng, Y.-C.; Blankenship, R. E.; Fleming, G. R. Evidence for Wavelike Energy Transfer Through Quantum Coherence in Photosynthetic Systems. *Nature* **2007**, *446*, 782–786.

(4) Lee, H.; Cheng, Y.-C.; Fleming, G. R. Coherence Dynamics in Photosynthesis: Protein Protection of Excitonic Coherence. *Science* **2007**, *316*, 1462–1465.

(5) Mirkovic, T.; Doust, A. B.; Kim, J.; Wilk, K. E.; Curutchet, C.; Mennucci, B.; Cammi, R.; Curmib, P. M. G.; Scholes, G. D. Ultrafast Light Harvesting Dynamics in the Cryptophyte Phycocyanin 645. *Photochem. Photobiol. Sci.* **2007**, *6*, 964–975.

(6) Scholes, G. D. Quantum-Coherent Electronic Energy Transfer: Did Nature Think of It First?. *J. Chem. Phys. Lett.* **2010**, *1*, 2–8.

(7) Jang, S.; Newton, M. D.; Silbey, R. J. Multichromophoric Förster Resonance Energy Transfer. *Phys. Rev. Lett.* **2004**, *92*, 218301/1–218301/4.

(8) Jang, S.; Netwton, M. D.; Silbey, R. J. Multichromophoric Förster Resonance Energy Transfer from B800 to B850 in the Light Harvesting Complex 2: Evidence for Subtle Energetic Optimization by Purple Bacteria. *J. Phys. Chem. B* **2007**, *111*, 6807–6814.

(9) Heijs, D. J.; Malyshev, V. A.; Knoester, J. Decoherence of Excitons in Multichromophore Systems: Thermal Line Broadening and Destruction of Superradiant Emission. *Phys. Rev. Lett.* **2005**, *95*, 177402/1–177402/4.

(10) Schröder, M.; Kleinekathöfer, U.; Schreiber, M. Calculation of Absorption Spectra for Light-Harvesting Systems Using Non-Markovian Approaches as well as Modified Redfield Theory. *J. Chem. Phys.* **2006**, *124*, 084903/1–084903/14.

(11) Palmieri, B.; Abramavicius, D.; Mukamel, S. Lindblad Equations for Strongly Coupled Populations and Coherences in Photosynthetic Complexes. *J. Chem. Phys.* **2009**, *130*, 204512/1–204512/10.

(12) Olaya-Castro, A.; Fan-Lee, C.; Fassioli-Olsen, F.; Johnson, N. F. Efficiency of Energy Transfer in a Light-Harvesting System Under Quantum Coherence. *Phys. Rev. B* **2008**, *78*, 085115/1–085115/7.

(13) Cheng, Y. C.; Silbey, R. J. Markovian Approximation in the Relaxation of Open Quantum Systems. *J. Phys. Chem. B.* **2005**, *109*, 21399–21405.

(14) Huo, P.; Coker, D. F. Iterative Linearized Density Matrix Propagation for Modeling Coherent Excitation Energy Transfer in Photosynthetic Light Harvesting. *J. Chem. Phys.* **2010**, *133*, 184108/1–184108/2.

(15) Ishizaki, A.; Fleming, G. R. On the Adequacy of the Redfield Equation and Related Approaches to the Study of Quantum Dynamics in Electronic Energy Transfer. *J. Chem. Phys.* **2009**, *130*, 234110/1–234110/9.

(16) Ishizaki, A.; Fleming, G. R. Unified Treatment of Quantum Coherent and Incoherent Hopping Dynamics in Electronic Energy Transfer: Reduced Hierarchy Equation Approach. *J. Chem. Phys.* **2009**, *130*, 234111/1–234111/10.

(17) Ishizaki, A.; Fleming, G. R. Theoretical Examination of Quantum Coherence in a Photosynthetic System at Physiological Temperature. *Proc. Natl. Acad. Sci. U.S.A.* **2009**, *106*, 17255–17260.

(18) Sarovar, M.; Ishizaki, A.; Fleming, G. R.; Whaley, K. B. Quantum Entanglement in Photosynthetic Light-Harvesting Complexes. *Nat. Phys.* **2010**, *6*, 462–467.

(19) Wu, J.; Liu, F.; Shen, Y.; Cao, J.; Silbey, R. J. Efficient Energy Transfer in Light-Harvesting Systems, I: Optimal Temperature, Reorganization Energy, and Spatial-Temporal Correlations. *New J. Phys.* **2010**, *12*, 105012/1–105012/17.

(20) Tao, G.; Miller, W. H. Semiclassical Description of Electronic Excition Population Transfer in a Model Photosynthetic System. *J. Phys. Chem. Lett.* **2010**, *1*, 891–894.

(21) Zhang, W. M.; Meier, T.; Chernyak, V.; Mukamel, S. Exciton-Migration and Three-Pulse Femtosecond Optical Spectroscopies of Photosynthetic Antenna Complexes. *J. Chem. Phys.* **1998**, *108*, 7763–7714.

(22) Yang, M.; Fleming, G. R. Influence of Phonons on Exciton Transfer Dynamics: Comparison of the Redfield, Förster, and Modified Redfield Equations. *Chem. Phys.* **2002**, *282*, 163–180.

(23) Pomyalov, A.; Tannor, D. The Non-Markovian Quantum Master Equation in the Collective-Mode Representation: Application to Barrier Crossing in the Intermediate Friction Regime. *J. Chem. Phys.* **2005**, *123*, 204111/1–204111/11.

(24) Dunkel, E. R.; Bonella, S.; Coker, D. F. Iterative Linearized Approach to Nonadiabatic Dynamics. *J. Chem. Phys.* **2008**, *129*, 114106/1–114106/15.

(25) Bonella, S.; Coker, D. F. LAND-map, a Linearized Approach to Non-Adiabatic Dynamics using the Mapping Formalism. *J. Chem. Phys.* **2005**, *122*, 194102/1–194102/13.

(26) Bonella, S.; Montemayor, D.; Coker, D. F. Linearized Path Integral Approach for Calculating Nonadiabatic Time Correlation Functions. *Proc. Natl. Acad. Sci* **2005**, *102*, 6715–6719.

(27) Huo, P.; Bonella, S.; Chen, L.; Coker, D. F. Linearized Approximations for Condensed Phase Non-Adiabatic Dynamics: Multi-Layered Baths and Brownian Dynamics Implementation. *Chem. Phys.* **2010**, *370*, 87–97.

(28) Spear-Bernstein, L.; Miller, K. R. Unique Location of the Phycobiliprotein Light-Harvesting Pigment in the Cryptophyceae. *J. Phycol.* **1989**, *25*, 412–419.

(29) Plenio, M. B.; Huelga, S. F. Dephasing-Assisted Transport: Quantum Networks and Biomolecules. *New J. Phys.* **2008**, *10*, 113019/1–113019/14.

(30) Caruso, F.; Chin, A. W.; Datta, A.; Huelga, S. F.; Plenio, M. B. Highly Efficient Energy Excitation Transfer in Light-Harvesting Complexes: The Fundamental Role of Noise-Assisted Transport. *J. Chem. Phys.* **2009**, 131105106/1–105106/15.

(31) Chin, A. W.; Datta, A.; Caruso, F.; Huelga, S. F.; Plenio, M. B. Noise-Assisted Energy Transfer in Quantum Networks and Light-Harvesting Complexes. *New J. Phys.* **2010**, *12*, 065002/1–065002/16.

(32) Cao, J.; Silbey, R. J. Optimization of Exciton Trapping in Energy Transfer Processes. *J. Phys. Chem. A* **2009**, *113*, 13826–13838.

(33) Ishizaki, A.; Fleming, G. R. Quantum Superpositions in Photosynthetic Light Harvesting: Delocalization and Entanglement. *New J. Phys.* **2010**, *12*, 055004/1–055004/13.

(34) Nalbach, P.; Eckel, J.; Thorwart, M. Quantum Coherent Biomolecular Energy Transfer with Spatially Correlated Fluctuations. *New J. Phys.* **2010**, *12*, 065043/1–065043/18.